Application of the Tersoff interatomic potential to pressure-induced polyamorphism of silicon

Renji Mukuno and Manabu Ishimaru*

[1]*Department of Materials Science and Engineering, Kyushu Institute of Technology, Kitakyushu, Fukuoka 804-8550, Japan*

Abstract

Molecular-dynamics simulations of pressure-induced structural changes in amorphous Si were performed by using the Tersoff interatomic potential, in order to examine the validity of this potential. The amorphous Si with a tetrahedral network was prepared by melt-quenching methods, and then it was compressed under the isothermal-isobaric conditions. It was found that the changes of atomic pair-distribution functions and static structure factors with increasing pressure are in agreement with those observed experimentally. The pressure-induced amorphous structures contained the short-range order similar to β-tin and *Imma* structures. These results suggested that the Tersoff potential is useful for describing the structural changes of amorphous Si under high pressure.

*To whom correspondence should be addressed. E-mail: ishimaru@post.matsc.kyutech.ac.jp

I. Introduction

Amorphous silicon (*a*-Si) is widely utilized not only as device applications but also as manufacturing technologies in the current semiconductor industries. For example, *a*-Si is an important semiconductor material applied to solar cells and thin film transistors. Recrystallization of *a*-Si on a single crystalline substrate, so-called solid phase epitaxy, is often applied for recovering the crystallinity and activating ion implanted dopants. When Si is used as an anode material for lithium-ion batteries, amorphization occurs during charging (lithiation). Since the atomic configurations strongly affect the material properties and processing, knowledge of atomistic structures of *a*-Si and its stability is required.

Molecular dynamics (MD) simulation is a powerful technique for investigating static and dynamic properties of materials at the atomic scale. The first principle (*ab initio*) MD method is highly accurate calculations, but are limited to short-time simulations of small systems due to the huge amount of calculation. Several empirical interatomic potentials have been proposed so far for large-scale and long-time MD simulations [1]. These potentials are set so as to reproduce the physical properties of the crystalline state, and are not optimized for the amorphous state. Therefore, it is necessary to examine the validity of the potential for the investigations of *a*-Si. The Stillinger-Weber potential consists of two- and three-body terms, and the latter is set to zero at the tetrahedral angle to stabilize the diamond structure [2]. *a*-Si networks were successfully generated by melt-quenching using this potential, but the three-body interaction has to be artificially strengthened during cooling process in order to stabilize the tetrahedral structure [3]. Another potential for Si proposed by Tersoff is expressed as a pairwise interaction, but the attractive term depends on the local environment which essentially includes many-body interactions [4]. Although this potential is overestimated the melting temperature of Si, *a*-Si networks can be produced without any *ad hoc* procedures during melt-quenching [5-7].

In the present study, we paid attention to an amorphous-to-amorphous phase transformation, so-called polyamorphism [8-14]. *a*-Si possesses the tetrahedrally-coordinated amorphous network at ambient pressure and exhibit a semiconducting property. On the other hand, the coordination number increases with pressure and finally high-density *a*-Si with metallic properties is formed. Ivashchenko *et al.* [15] investigated the amorphous structures of Si_xC_{1-x} alloys after pressure-induced phase transformation by the MD simulations based on the Tersoff potential, but the detail structural changes of *a*-Si were not well understood. Here, we examined the structural changes during pressurizing, and confirmed the validity of the Tersoff potential for the investigations of pressure-induced polyamorphism in *a*-Si.

II. Simulation procedures

a-Si networks were prepared by melt-quenching methods, as described elsewhere [7]. 2744 or 4096 Si atoms interacting by the Tersoff interatomic potential were initially arranged on a diamond structure with a size of $7a_0$x$7a_0$x$7a_0$ or $8a_0$x$8a_0$x$8a_0$, respectively, where a_0 is an initial lattice parameter of the unit cell, 5.43 Å. The former MD cell was used for examining the effects of pressure rates on the density change, while the latter one was used for characterizing the pressure-induced structures of *a*-Si. The periodic boundary conditions were applied in all directions. This MD cell was heated up by velocity scaling methods, and maintained at 5000 K for 100 ps in order to produce liquid Si in a steady state. The obtained liquid was then quenched to 300 K with a cooling rate of 10^{12} K/s, and maintained at this temperature for 10 ps. The simulations were performed under the isobaric condition, and the equations of motion were integrated using the velocity form of the Verlet algorithm with a time step of Δt = 2 fs.

To examine pressure-induced polyamorphism, a compressive pressure up to 30 GPa was applied to the as-quenched *a*-Si under the isothermal and isobaric conditions, so-called *NPT* ensemble. For the simulations based on the *NPT* ensemble, a Nosé-Hoover barostat was

used. The velocity of each atom was scaled every time step, while the time constant to control the pressure was set to be 10 ps (5000 time steps). All MD simulations were carried out with an MD open-source code, Large-scale Atomic/Molecular Massively Parallel Simulator (LAMMPS) [16].

III. Results and discussion

The density of as-quenched *a*-Si obtained here was 2.26 g/cm^3, 3.0% lower than that of crystalline Si, which is in agreement with the experimental result (1.8% - 3.1%) [17,18]. Figure 1 shows the density change under compression with different pressure rates at 300 K. A linear increase of the density is initially observed, while the slope changes at a certain pressure. For example, the slope becomes large between ~18 and ~25 GPa at a pressure rate of 25 Pa/fs. This suggests that a pressure-induced structural change occurs. The phase transformation pressure shifts to the lower pressure side with decreasing the pressure rate. The *a*-Si compressed to 30 GPa with a pressure rate of 25 Pa/fs were decompressed by the same pressure rate. It was confirmed that the density decreases by decompression, but it does not return to the initial value (2.26 g/cm^3). This means that the pressure-induced structural change is the first-order phase transformation and considerable hysteresis exists, as observed previously [12].

Atomic configurations generated by melt-quenching methods possessed a tetrahedral network and successfully reproduced the structural features of *a*-Si, as reported previously [5-7]. Figure 2(a) shows atomic pair-distribution functions, $g(r)$, of atomic configurations obtained by applying the compressive pressure at 300 K for 500 ns. The first and second peaks located at 2.36 and 3.86 Å, respectively, in the $g(r)$ of as-quenched *a*-Si move to the shorter distance side at 15 GPa. The shape of the $g(r)$ is almost the same as that of the as-quenched *a*-Si up to 17.5 GPa, but a shoulder appears at the shorter distance side of the second peak. The first peak shifts to the longer distance side at ≥20 GPa. The second peak starts to split and eventually a

new peak at 3.06 Å becomes dominant at 25 GPa. The structural changes in Fig. 2(a) are in good agreement with those obtained by previous x-ray diffraction experiments [11] and *ab initio* MD simulations [14].

The average coordination number was calculated by integrating $4\pi r^2\rho_0 g(r)$ up to the first minimum of the $g(r)$, where ρ_0 is the number density. Since the number of bonds per atom suddenly increases between 17.5 and 20 GPa (see the inset of Fig. 2(a)), the interatomic distance increases as observed in the $g(r)$ of Fig. 2(a). It has been reported that the coordination number changes from 4 to 6 with increasing the compressive pressure, and a low density amorphous to high density amorphous transformation is induced by applying compressive pressure [10-14]. This result is in agreement with the present study.

To compare with the available experimental data, the static structure factors, $S(Q)$, were calculated by Fourier transforming $g(r)$,

$$S(Q) = 1 + 4\pi\rho_0 \int_0^\infty r^2\{g(r) - 1\}\frac{\sin Qr}{Qr}dr.$$

Here, ρ_0 is the average number density of atoms, Q is the scattering vector. The resultant $S(Q)$ is shown in Fig. 2(b). The ripple on the low-Q side of the first peak is due to a truncation error and should be disregarded. The $S(Q)$ of as-quenched *a*-Si is in good agreement with that obtained experimentally [19-22]. The peaks move to higher-Q with increasing the pressure, and the first peak remarkably shifts at 20 GPa. In addition, the peak height of the first peak becomes larger than that of the second peak by pressurizing. The results of Fig. 2(b) well reproduce the behavior of $S(Q)$ obtained experimentally [11], suggesting the validity of the present MD simulations.

Three-body correlations, so called bond-angle distribution functions, $g(\theta)$, were calculated. A bond was defined as the bond length of the first minimum between the first and second peaks of the $g(r)$. Figure 3 shows the $g(\theta)$ of amorphous networks as a function of pressure. A peak of the $g(\theta)$ obtained from the as-quenched *a*-Si exists at the ~110°, in

agreement with the tetrahedrally-coordinated amorphous network. Upon pressurization, additional peaks appear at ~60^{o} and ~80^{o}, and finally the latter becomes the main peak. A similar structure was observed in MD simulation of nanoindentation on a (100) oriented silicon surface using the Tersoff potential [23,24]. Kugler and Várallyay [25,26] examined possible atomic arrangements in the structure of *a*-Si based on the Cambridge Structural Database, and pointed out that the peaks in the interval 75^{o}-96^{o} and around 60^{o} can exist as minor atomic configurations in *a*-Si networks. Our simulations revealed that these inherent configurations become more pronounced by pressurizing.

The shape of $g(r)$ and $g(\theta)$ starts to change at 17.5 GPa, and it was confirmed that the change becomes more pronounced with increasing the simulation time. This indicates that an amorphous-to-amorphous structural phase transformation progresses at this pressure. Ivashchenko *et al.* [15] examined pressure-induced structural changes of *a*-Si generated by the Tersoff potential, and observed a significant change in $g(\theta)$ at ~9 GPa. This value is much smaller than that observed in the present study, and the reason is unclear. However, our result is in agreement with an *ab initio* MD result (16.25 GPa) [12], suggesting the validity of the Tersoff potential.

It was confirmed that the MD simulations based on the Tersoff interatomic potential can reproduced the pressure-induced structural changes of *a*-Si obtained by x-ray diffraction experiments and *ab initio* MD simulations, suggesting the validity of the present study. We examined the detailed structures as a function of coordination numbers. Figure 4 shows the time evolution of each coordination number: (a) 15 GPa, (b) 20 GPa, and (c) 25 GPa. It is apparent that the fourfold coordinated atoms are dominant at 15 GPa, indicating that the tetrahedral amorphous network is maintained. On the other hand, the amount of over-coordinated atoms, such as five and six coordination, increases with the time in Figs. 4(b) and 4(c), but the structural change is not completed in the present time scale (<500 ns). Interestingly, the fivefold

coordinated atoms decrease after taking a maximum value at ~80 ns at 25 GPa. This suggests that several local minima exist for atomic configurations of pressure-induced amorphous networks.

Bond-angle distribution functions around an atom with *i*-fold coordination, $g_i(\theta)$, were calculated. The cutoff distance is defined as the first minimum of the pair-distribution function for each coordinated atom, which corresponds to 2.70, 2.74, and 2.78 Å for the four-, five-, and six-fold coordinated atoms, respectively. Figure 5 shows the $g_i(\theta)$ of atomic configurations after pressurizing at 25 GPa for 500 ns. Here, we show the profiles corresponding to the coordination number with the existence probability of >10%. The $g_4(\theta)$ possesses a peak at ~110^o, indicating that the tetrahedral structure is maintained around the four-fold coordinated atom. On the other hand, prominent peaks and shoulder exist in the $g_5(\theta)$ and $g_6(\theta)$.

It is known that the diamond structure of crystalline Si (space group: $Fd\bar{3}m$; lattice parameter: a = 5.430 Å at ambient pressure) transforms to the β-tin structure ($I4_1/amd$; a = 4.690 Å, c = 2.578 Å [27]) under high pressure [28]. A previous study has pointed out that the pressure-induced *a*-Si networks contain a similar short-range order to β-tin structure [14]. The bond lengths of the β-tin structure are 2.432, 2.578, and 3.03 Å, in agreement with the peak locations of the $g(r)$ obtained by 25 GPa (Fig. 2(a)). Solid lines in Fig. 5 denote the bond angles within the first coordination shell of crystalline Si with a β-tin structure. It should be noted that the bond angle of ~60^o cannot be explained by β-tin structure. It has been reported that the β-tin phase transforms to another metastable phase (*Imma*; a = 4.737 Å, b = 4.502 Å, c = 2.550 Å [29]) by further pressure. The bond angles of the *Imma* structure (broken lines) are in agreement with the $g_6(\theta)$ profile, though the coordination number of the *Imma* structure is 8. There are structural and energetic similarities between β-tin and *Imma* phases [30], and therefore it is thought that the pressure-induced *a*-Si networks contain a similar short-range

order to β-tin and *Imma* structures. The latter structure becomes dominant with increasing the compressive pressure.

IV. Conclusions

The pressure-induced structural changes of *a*-Si were examined by MD simulations using the Tersoff interatomic potential. The density of *a*-Si linearly increased with pressure, while the tetrahedrally-coordinated structures were maintained. On the other hand, the coordination number increased with pressure and finally high-density *a*-Si was formed. The changes of atomic pair-distribution functions and static structure factor with increasing pressure were in agreement with those obtained experimentally, suggesting the validity of the Tersoff potential for analyzing pressure-induced polyamorphism of Si. Bond angle distribution functions revealed that the pressure-induce a-Si possesses short-range order similar to β-tin and *Imma* structures.

Acknowledgements

This work was supported in part by Grant-in-Aid for Scientific Research (B) (Grant No. 19H02463) from the Ministry of Education, Sports, Science, and Technology, Japan.

References

[1] For example, see S. J. Cook and P. Clancy, Phys. Rev. B **47**, 7686 (1993).

[2] F. H. Stillinger and T. A. Weber, Phys. Rev. B **31**, 5262 (1985): Erratum **33**, 1451 (1986).

[3] W. D. Luedtke and U. Landman, Phys. Rev. B **37**, 4656 (1988).

[4] J. Tersoff, Phys. Rev. B **39**, 5566 (1989).

[5] M. Ishimaru, S. Munetoh, and T. Motooka, Phys. Rev. B **56**, 15133 (1997).

[6] M. Ishimaru, J. Appl. Phys. **91**, 686 (2002).

[7] K. Kohno and M. Ishimaru, Jpn. J. Appl. Phys. **57**, 095503 (2018).

[8] P. H. Poole, T. Grande, C. A. Angell, and P. F. McMillan, Science **275**, 322 (1997).

[9] S. K. Deb, M. Wilding, M. Somayazulu, P. F. McMillan, Nature **414**, 528 (2001).

[10] P. F. McMillan, M. Wilson, D. Daisenberger, and D. Machon, Nature Mater. **4**, 680 (2005).

[11] D. Daisenberger, M. Wilson, P. F. McMillan, R. Q. Cabrera, M. C. Wilding, and D. Machon, Phys. Rev. B **75**, 224118 (2007).

[12] M. Durandurdu and D. A. Drabold, Phys. Rev. B **64**, 014101 (2001).

[13] T. Morishita, Phys. Rev. Lett. **93**, 055503 (2004).

[14] T. Morishita, J. Chem. Phys. **130**, 194709 (2009).

[15] V. I. Ivashchenko, P. E. A. Turchi, V. I. Shevchenko, L. A. Ivashchenko, and O. A. Shramko, Phys. Rev. B **71**, 165209 (2005).

[16] S. Plimpton, J Comput. Phys. **117**, 1 (1995): http://lammps.sandia.gov/

[17] J. S. Custer, M. O. Thompson, D. C. Jacobson, J. M. Poate, S. Roorda, W. C. Sinke, and S. Spaepen, Appl. Phys. Lett. **64**, 437 (1994).

[18] P. K. Giri, V. Raineri, G. Franzo, and E. Rimini, Phys. Rev. B **65**, 012110 (2001).

[19] J. Fortner and J. S. Lannin, Phys. Rev. B **39**, 5527 (1989).

[20] S. Kugler, G. Molnár, G. Petö, E. Zsoldos, L. Rosta, A. Menelle, and R. Bellissent, Phys.

Rev. B **40**, 8030 (1989).

[21] K. Laaziri, S. Kycia, S. Roorda, M. Chicoine, J. L. Robertson, J. Wang, and S. C. Moss, Phys. Rev. B **60**, 13520 (1999).

[22] L. Pusztai and S. Kugler, J. Phys.: Condens. Matter **17**, 2617 (2005).

[23] J. Han, S. Xu, J. Sun, L. Fang, and H. Zhu, RSC Adv. **7**, 1357 (2017).

[24] V. I. Ivashchenko, P. E. A. Turchi, and V. I. Shevchenko, Phys. Rev. B **78**, 035205 (2008).

[25] S. Kugler and Z. Várallyay, Philos. Mag. Lett. **81**, 569 (2001).

[26] Z. Várallyay and S. Kugler, J. Non-Cryst. Solids **299-302**, 265 (2002).

[27] J. Z. Hu, L. D. Merkle, C. S. Menoni, and I. L. Spain, Phys. Rev. B **34**, 4679 (1986).

[28] T. Soma, H. Iwanami, and H. Matsuo, Solid State Commun. **42**, 469 (1982).

[29] M. I. McMahon and R. J. Nelmes, Phys. Rev. B **47**, 8337 (1993).

[30] S. M. Sharma and S. K. Sikka, J. Phys. Chem. Solids **46**, 477 (1985).

Figure captions

Figure 1. Density changes of *a*-Si during compression and decompression with different pressure rates: 25, 50, and 500 Pa/fs. The density linearly increases with pressure, but the slop changes at a certain pressure and its position moves toward the higher pressure with increasing pressure rate. The *a*-Si compressed to 30 GPa with a pressure rate of 25 Pa/fs were decompressed by the same pressure rate.

Figure 2. (a) Atomic pair-distribution functions, $g(r)$, and (b) structure factors, $S(Q)$, as a function of compressive pressure. "0 GPa" means as-quenched amorphous Si. The $S(Q)$ were calculated by Fourier transform of the $g(r)$. The inset of (a) is the coordination number as a function of pressure.

Figure 3. Bond angle distribution functions, $g(\theta)$, as a function of compressive pressure. The atomic configurations after pressurizing at 300 K for 500 ns were analyzed. A bond was defined as the first minimum of $g(r)$ of Fig. 2(a).

Figure 4. Time dependence of each coordination number under pressure. (a) 15, (b) 20, and (c) 25 GPa. The coordination numbers with the existence probability of >1% are plotted.

Figure 5. (a,b) Bond-angle distribution functions around an atom with *i*-fold coordination in the atomic configurations after pressurizing at 25 GPa for 500 ns. Solid lines (~75°, ~94°, ~105°, ~150°) and broken lines (~60°, ~77°, ~100°, ~115°, ~135°, ~155°) denote the bond angles within the first coordination shell of crystalline Si with β-tin and *Imma* structures, respectively.

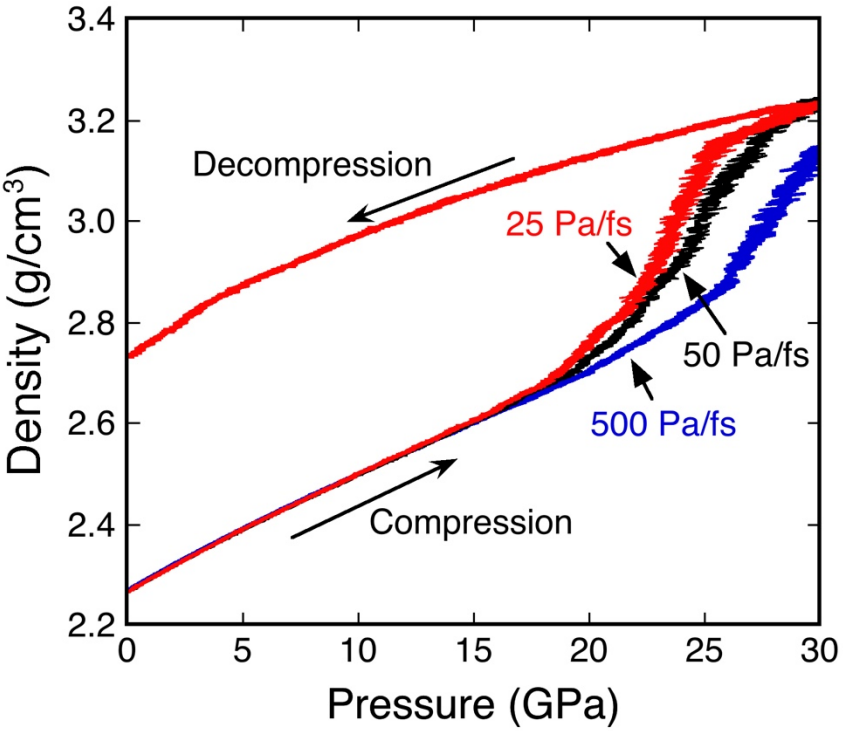
Density (g/cm^3)
Pressure (GPa)
Decompression
Compression
25 Pa/fs
50 Pa/fs
500 Pa/fs
3.4
3.2
3.0
2.8
2.6
2.4
2.2
0
5
10
15
20
25
30

Fig. 1

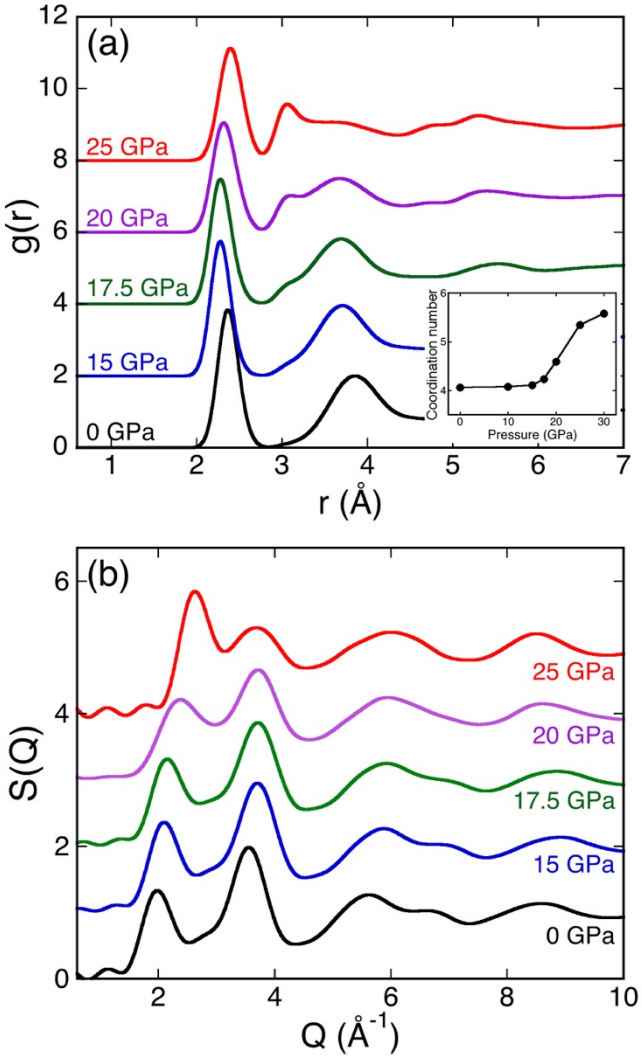
(a)
25 GPa
20 GPa
17.5 GPa
15 GPa
0 GPa
g(r)
r (Å)
Coordination number
Pressure (GPa)
(b)
25 GPa
20 GPa
17.5 GPa
15 GPa
0 GPa
S(Q)
Q (Å^{-1})

Fig. 2

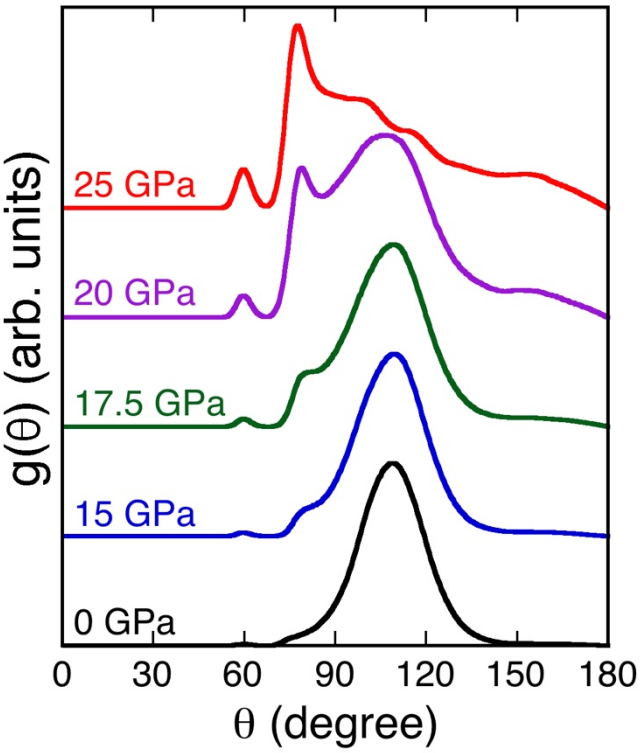
25 GPa
20 GPa
17.5 GPa
15 GPa
0 GPa
g(θ) (arb. units)
0
30
60
90
120
150
180
θ (degree)

Fig. 3

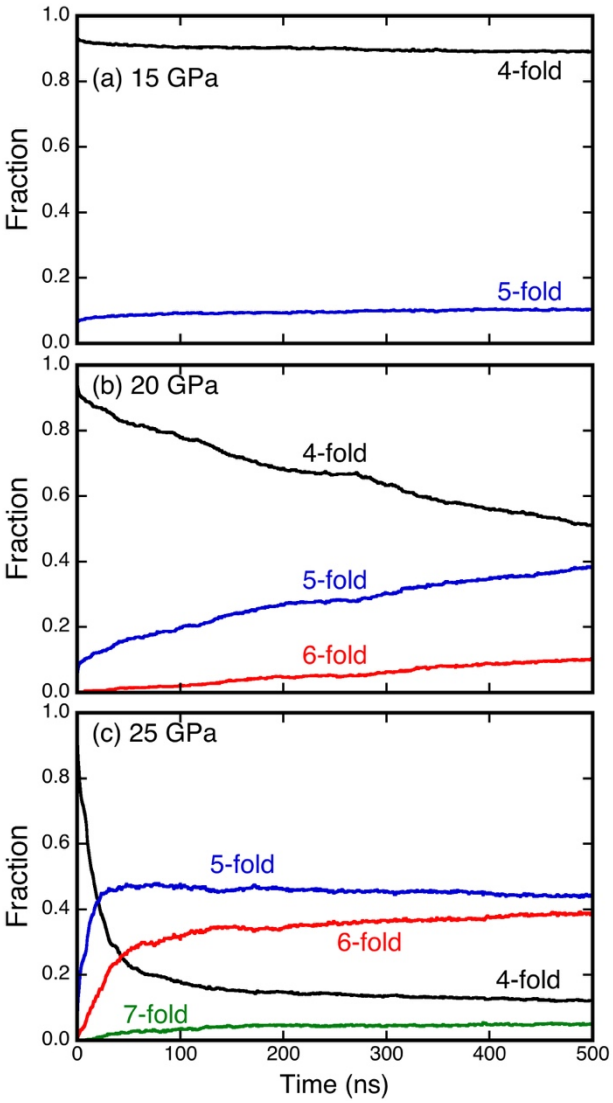
(a) 15 GPa
4-fold
5-fold
(b) 20 GPa
4-fold
5-fold
6-fold
(c) 25 GPa
5-fold
6-fold
4-fold
7-fold
Fraction
Time (ns)
0.0
0.2
0.4
0.6
0.8
1.0
0
100
200
300
400
500

Fig. 4

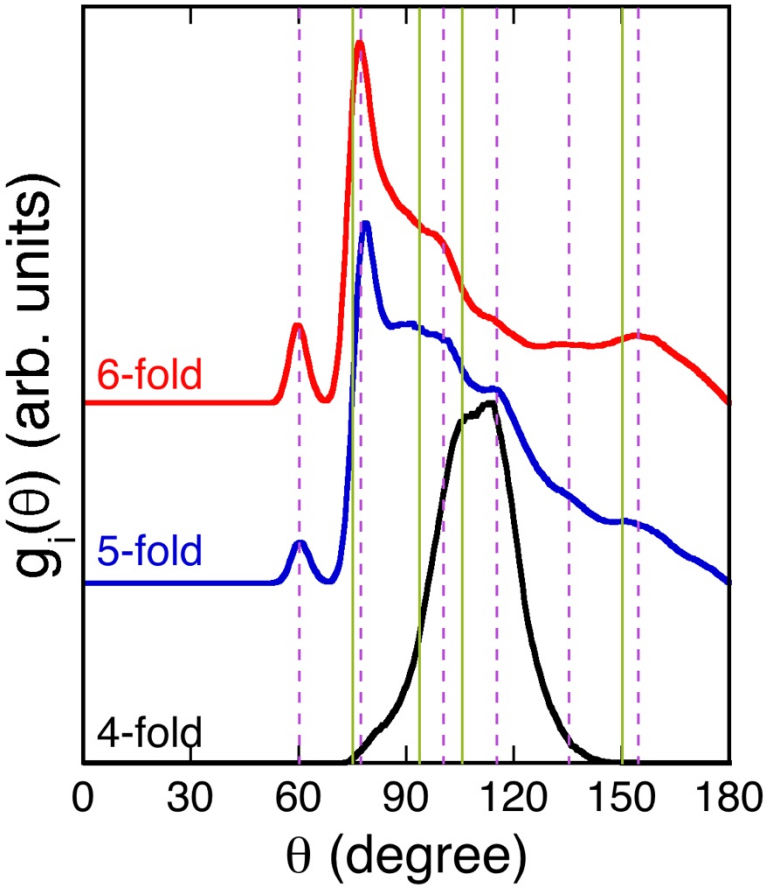
6-fold
5-fold
4-fold
$g_i(\theta)$ (arb. units)
0
30
60
90
120
150
180
θ (degree)

Fig. 5